Research report

Near-infrared vibrational overtone spectra of teepleite, $Na_2B(OH)_4Cl$, and its deutero analog

Christian Reber
Département de chimie
Université de Montréal
C.P. 6128, Succ. Centre-ville
Montréal QC H3C 3J7, Canada

Paul J. McCarthy
Department of Chemistry
Canisius College
Buffalo, NY 14208, USA

Ian M. Walker
Department of Chemistry
York University
Toronto ON M3J 1P3, Canada

Correspondence:
Christian Reber, christian.reber@umontreal.ca

Submitted to papyrus.umontreal.ca on December 5, 2021

Abstract

Single crystals of the naturally occurring mineral teepleite, $Na_2B(OH)_4Cl$, and its deuterated analog were grown and their polarized near-infrared absorption spectra recorded at 10 K. The spectra show three intense, sharp sets of O–H and O–D overtone transitions, spanning the range from 6000 cm^{-1} to 13000 cm^{-1}, approximately 1600 nm to 750 nm. Such detailed, well-resolved spectra are exceptional. Anharmonicities are determined and compared to literature values.

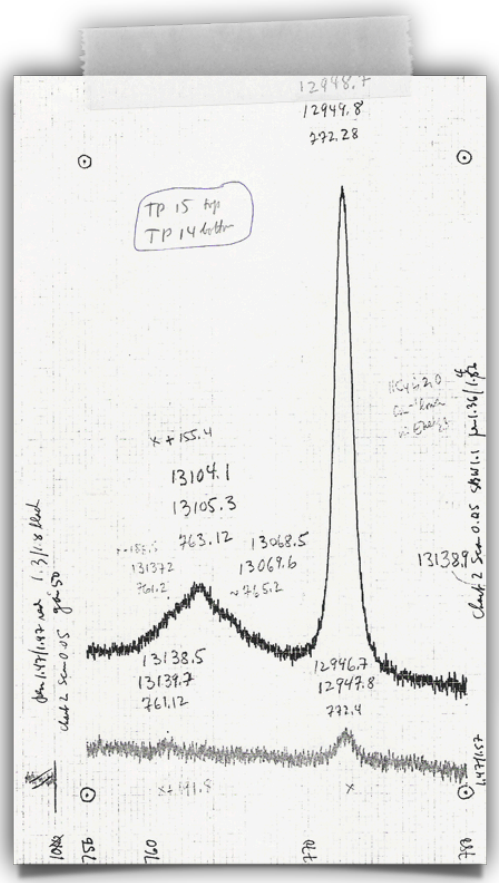

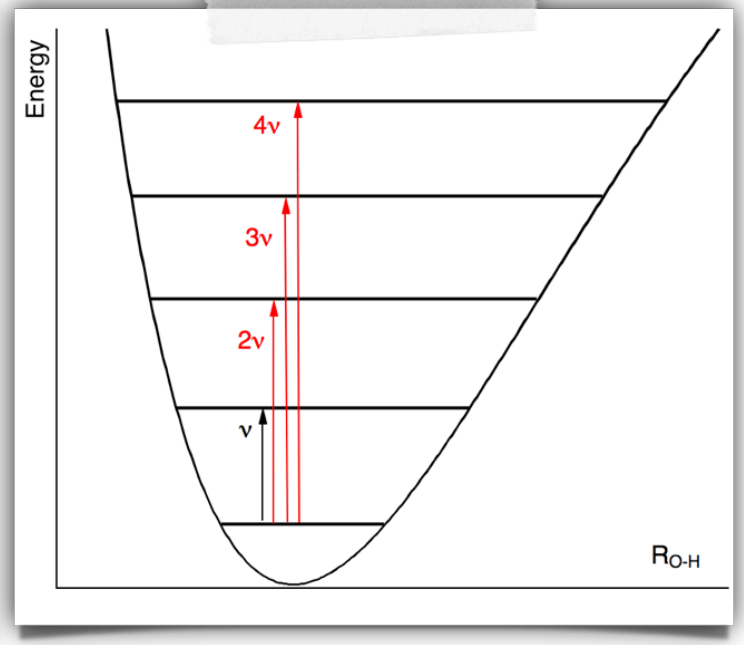

Introduction

The naturally occurring mineral teepleite, $Na_2B(OH)_4Cl$, is named in honor of John E. Teeple for his contributions to the knowledge of the chemistry of the Mojave desert's dry lakes (1). Its simple composition and structure of high symmetry make it an attractive solid for a study of the near-infrared (NIR) absorption spectrum, where vibrational overtone transitions of OH^- and OD^- anions are expected. The crystal structure of teepleite has been determined by X-ray diffraction (2) and is illustrated in Figure 1. It belongs to the tetragonal space group P4/nmm with a = 7.260 Å, c = 4.847 Å, Z = 2. The BO_4^{5-} group has a tetrahedral structure with the boron atom lying on a point of D_{2d} symmetry. All OH^- anions are equivalent and either in the *ac* or *bc* planes. Refined hydrogen positions are published; the O–H distance is 0.88 Å (2). The O–H···Cl hydrogen bond is nearly linear, with an angle of 176.1° and the O···Cl distance is 3.29 Å. This is similar, for example, to the O–H···Cl distances in $CsMnCl_3{\cdot}2\ H_2O$ (3.145 and 3.297 Å) (3) $M_2MnCl_4{\cdot}2H_2O$ (M: Rb, Cs, 3.17 to 3.29 Å) (4) $Cs_2CrCl_5{\cdot}4H_2O$ (3.006 and 3.062 Å) (5) and $Cs_3VCl_6{\cdot}4H_2O$ (3.038 Å) (6). H···Cl hydrogen bonds are shown as dotted lines in Figure 1, illustrating the extensive hydrogen bonding network throughout this structure.

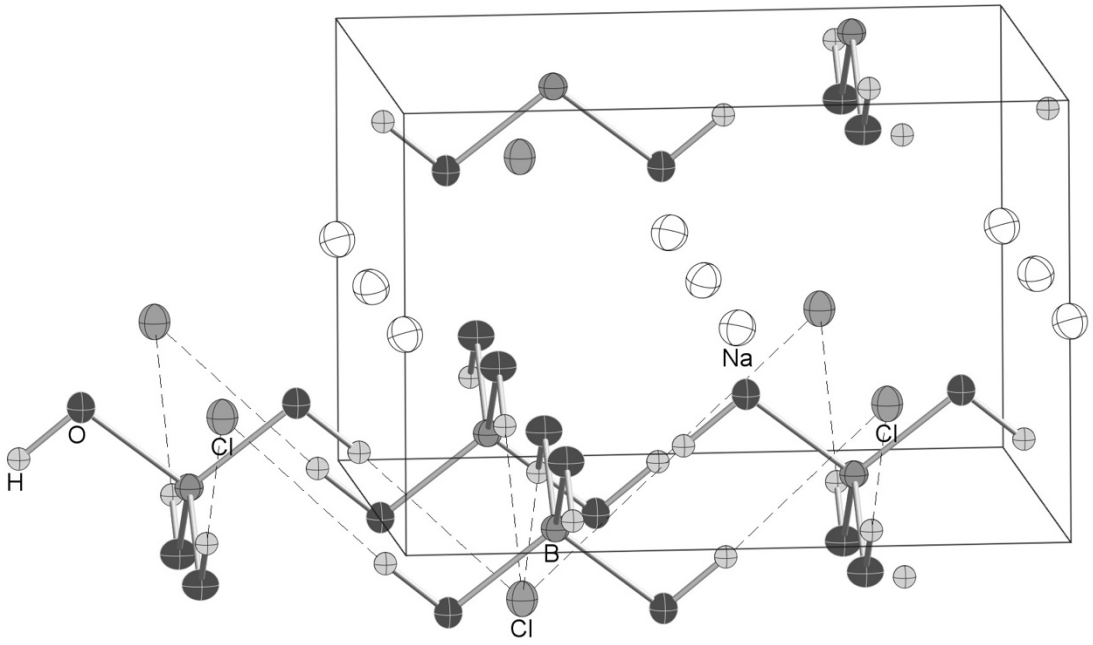

Figure 1. Tetragonal unit cell of teepleite. The crystal *c* axis is vertical, and the *a* axis horizontal in the plane of the Figure. Full $B(OH)_4^-$ units with H···Cl hydrogen bonds given as dotted lines are shown in the lower half of the unit cell.

Infrared and Raman spectra of teepleite have been published and discussed (7,8), with assignments of the vibrational modes both in the D_{2d} point group of the boron sites and its D_{4h} factor group. To the best of our knowledge, the NIR overtone spectra presented here have not been reported before. Overtone transition energies of high-frequency oscillators such as O–H have been used as benchmark experimental quantities to test sophisticated theoretical models (9) and to probe impurities in a variety of oxide materials (10). They are also an important factor determining nonradiative relaxation of luminophores, especially in the NIR (11). Such transitions often occur as broad, weak bands that are hard to measure. An insightful overview chapter summarizing an authoritative body of work on O–H and O–D stretching fundamental and first overtone frequencies of organic compounds gives an order of magnitude of 235-280 cm^{-1} for the width of these transitions at room temperature (12). It is therefore useful to study simple crystalline systems such as teepleite with well-oriented OH^- groups in order to observe narrower overtone transitions. Such diatomic motifs are attractive, as textbook models for diatomic molecules can be applied to obtain spectroscopic parameters and bonding information. The following is intended to provide an example of such a study at the advanced undergraduate level.

The anharmonicity of O–H stretching modes in the presence of hydrogen bonds is a classic area of spectroscopic studies, with vibrational overtone transitions in NIR absorption spectra providing key experimental information (12-14). The resolution of the spectra can be improved in several ways. We explore two of these possibilities: first, lowering the temperature, which leads to sharper observed transitions for most compounds, and second, choosing a structure with an oriented system of O–H bonds. All of our previous studies (3,4,15-20) of the O–H stretching frequency have involved water, in which the two contiguous O–H bonds will normally be rather strongly coupled. In teepleite, $Na_2B(OH)_4Cl$, there are four O–H bonds, each separated from the others by two intervening B–O bonds. This should reduce the coupling between the O–H oscillators. The spectra accordingly might be expected to be more like those of isolated OH^- anions. In addition, the rather high symmetry of the $B(OH)_4^-$ group may make the spectra less complex than those found in species of lower symmetry. The spectra are in fact quite unusual in that the O-H stretch and its overtones are exceptionally intense and sharp. This makes it possible to measure the second and third overtones, which are not usually visible in solid-state spectra, even at low temperature.

Experimental

An equimolar mixture of H_3BO_3, NaOH, and NaCl was dissolved in water, filtered, and left to evaporate. Robust, clear crystals formed slowly; many were square plates. Under crossed polarizers these plates show complete extinction. Since the material belongs to a tetragonal space group, the complete extinction indicates that the unique fourfold axis lies perpendicular to the plate. Highly deuterated crystals were prepared by dissolving the above crystals in D_2O and allowing the solution to evaporate in a desiccator over concentrated H_2SO_4. Crystals containing

about 50% deuterium were prepared in an analogous manner. Infrared spectra were recorded in Nujol or fluorolube mulls at room temperature using a Nicolet Impact 410 FTIR spectrophotometer equipped with OMNIC FTIR software. NIR spectra were recorded between September 1996 and July 1997 at Canisius College on a Varian-2300 spectrophotometer equipped with a Displex cryogenic refrigerator. The internal wavelength calibration on the Varian 2300 was used. The light was polarized by means of a pair of Glan-Thompson prisms. Axial spectra were recorded as well as those with the electric vector of the radiation parallel and perpendicular to the *c* axis of the crystal. Peak wavelengths were determined for all spectra and averaged for calculating the final wavenumber values.

Spectroscopic Results

Overtone absorption spectra of $Na_2B(OH)_4Cl$ in the NIR are shown in Figure 2. The IR spectrum of teepleite shows two sharp peaks in the O–H stretching region at 3538 and 3559 cm^{-1}, in very good agreement with the published IR frequencies of 3535 and 3565 cm^{-1} (8). The 2ν, 3ν and 4ν overtone bands are easily assigned from these frequencies, as shown in Figure 2. The highly deuterated species has corresponding IR bands at 2611 and 2628 cm^{-1}. For all crystals the axial NIR spectrum is identical with the E⊥*c* spectrum, as expected for electric dipole transitions. In the polarized NIR spectra the band positions and intensities differ in the two polarizations. For the O-H stretching modes, the combination bands in Figure 2a are more intense in E||*c* than in E⊥*c* polarization. In contrast, the 2ν, 3ν and 4ν overtone bands observed in E⊥*c* polarization are about 3 cm^{-1} higher in energy and are more intense than the bands in E||*c* polarization, as illustrated in Figures 2b, 2c and 2d. The energies of all observed O–H stretching overtone transitions in wavenumber (cm^{-1}) units are given in Table 1. Wavenumber differences $\Delta G(v+1/2)$ with v= 0,1,2,3 between adjacent transitions, as defined in the analysis below, are also given in the table. v denotes the vibrational quantum number of the lower-energy level used to calculate $\Delta G(v+1/2)$. These differences decrease with increasing quantum number v, as expected for anharmonic oscillators.

Table 1. Observed infrared and near-infrared peak positions for O–H and O–D stretching vibrations of teepleite and its deuterated analog. Differences $\Delta G(v+1/2)$ are given. Values are in wavenumber (cm^{-1}) units and are averages over all measured spectra.

Assignment	$Na_2B(OH)_4Cl$	$Na_2B(OD)_4Cl$
ν(v=0 → v=1) = $\Delta G_{1/2}$	3559	2628
$\Delta G_{3/2}$	3321	2492
2ν (v=0 → v=2)	6880	5120
$\Delta G_{5/2}$	3139	2407
3ν (v=0 → v=3)	10019	7527
$\Delta G_{7/2}$	2930	2301
4ν (v=0 → v=4)	12949	9828

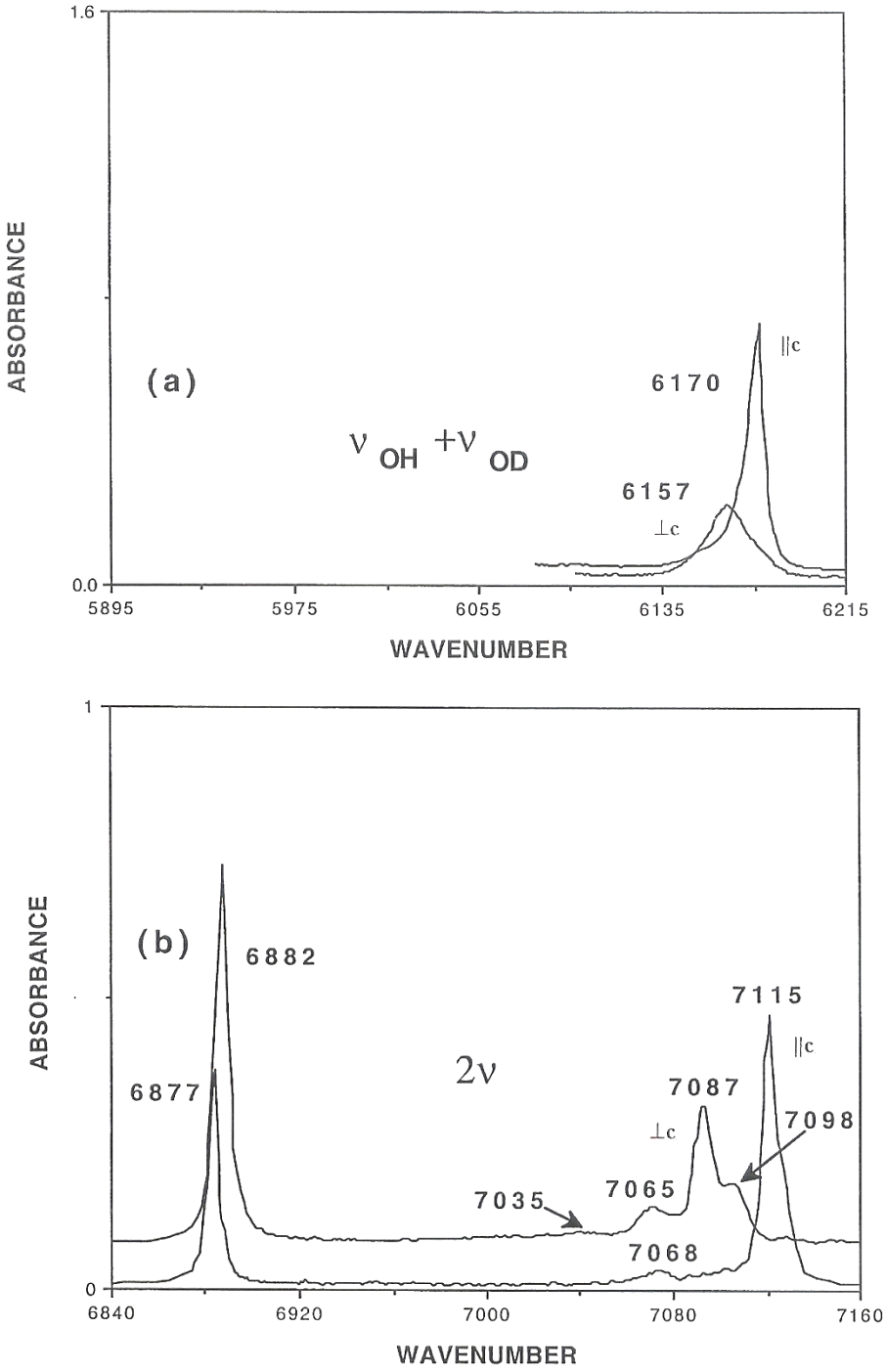

Figure 2. Hydroxyl stretch overtones of teepleite measured at 10 K with light polarized perpendicular and parallel to the crystal *c* axis. A wavenumber range of 320 cm^{-1} is used for (a) to (d). (a) was recorded on a 50% deuterated crystal, (b) to (d) on undeuterated crystals. Panels (b), (c), and (d) show the observed bands in the 2ν, 3ν, and 4ν wavenumber ranges. Band maxima are given in Table 1. The figure was made by digitizing suitable sections of the recorded spectra. These digitized spectra were then converted from wavelength to wavenumber abscissa units.

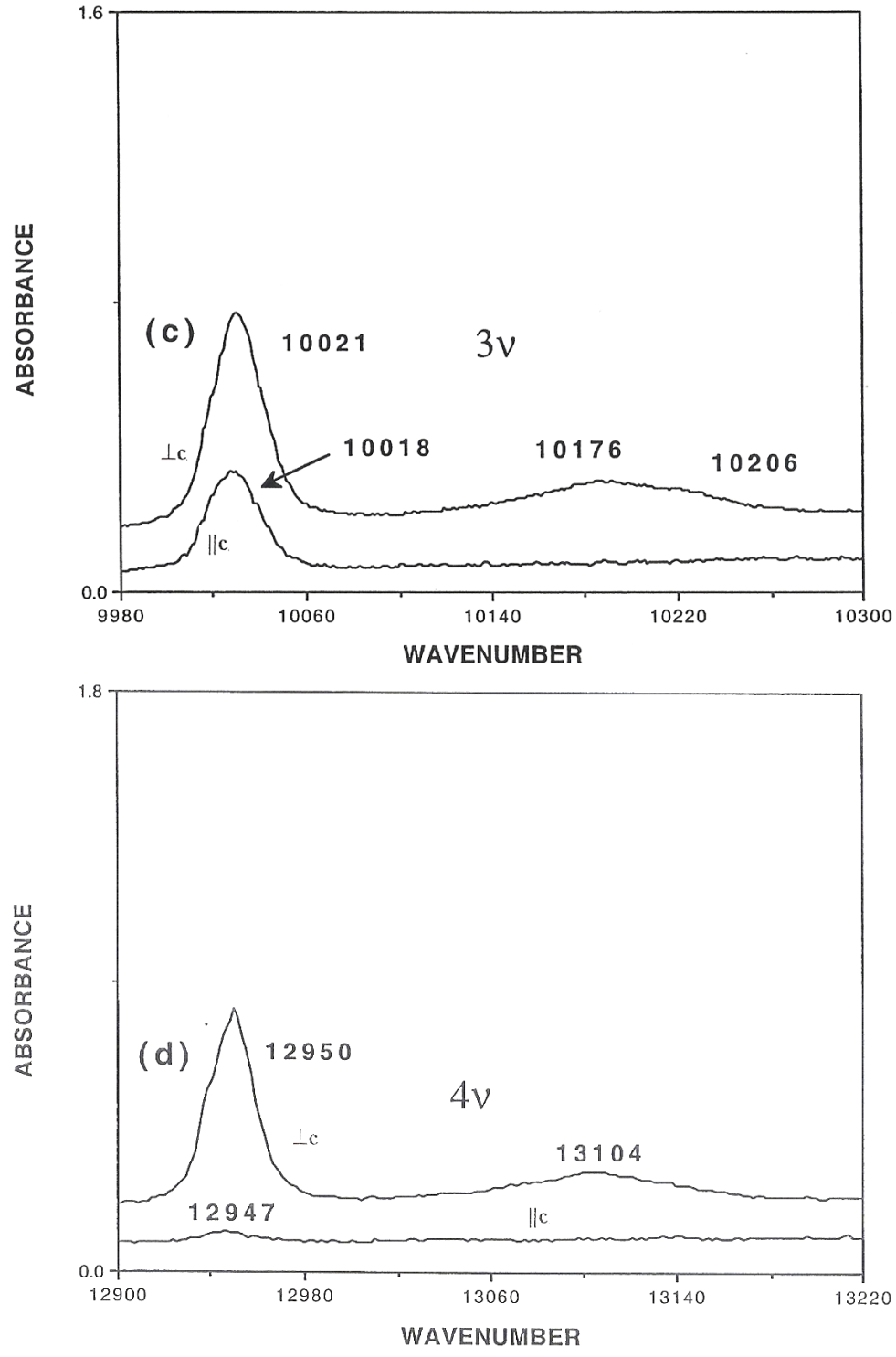

Figure 2. Continued.

Some intensity difference between polarizations is expected. If we assume that the O–H···Cl bond is linear, then from the positions of O and Cl in the crystal we calculate that the O–H vectors have *xy* and *z* components in a ratio of 1.41 to 1.00. The measured ratios ($\perp c/\|c$) are 2.0 (first overtone), 2.3 (second overtone), and 27.5 (third overtone); see Figure 2. The cause of the sharp decrease in intensity in the E$\|c$ polarization in the last pair is not known.

The width at half height of the overtone bands is 10 cm^{-1} for the combination bands in Figure 2a and the first overtone in Figure 2b, and 25 cm^{-1} for the second and third overtones in Figures 2c and 2d, respectively. These transitions are therefore narrower by at least an order of magnitude than the range given in (12), and comparable to those reported for matrix-isolated clusters of alcohol molecules at low temperature or doped crystals (12,13).

An unusual observation was made on the E$\|c$ spectrum. As the gain is increased, the overtone band at 6877 cm^{-1} becomes narrower, but also shifts slightly to higher energy. Between a gain of about 100 and a gain of 600-1200 the band appears to shift about 3 cm^{-1} to higher energy. The reason for this is not clear.

The contours of the 2ν spectra of the highly deuterated and the protiated species are very similar except for band positions and band separations. While the 2ν region shows both overtone and combination bands, the 3ν and 4ν regions show no evidence of combination bands. Presumably because of their weakness and greater multiplicity they cannot be seen above the background.

An interesting feature of the spectra is the weak bands slightly higher in energy than the overtone bands. In the E$\perp c$ spectrum these lie 92, 120, 153, 183, 205, 216, and 238 cm^{-1} above the first overtone (2ν) band and about 155 and 185 cm^{-1} above the second and third bands for the O–H spectra. Not all these bands are shown in Figure 2, but they were observed in various crystals. Similar bands are seen at 93 and 199 cm^{-1} in the 2ν region of the O–D E$\perp c$ spectrum. In the E$\|c$ spectra weak bands are seen 191 and 86 cm^{-1} above the first overtone in the O–H and O–D spectra. All these bands are probably hydrogen-bond modes, indicative of the significant influence of the crystal lattice on O–H vibrational modes.

Discussion

The overtone transitions in Figure 2 are both unusually intense and narrow. The high intensity is most likely due to interactions throughout the hydrogen bonding network illustrated in Figure 1. This increase has been documented and qualitatively discussed (12). The observed polarizations can not be rationalized in the D_{2d} point group of the $B(OH)_4^-$ anion with the rules given on p. 164 of (21), again indicating that interactions throughout the crystal lattice and low-frequency delocalized modes play an important role.

In the following, we analyze the overtone band energies with the anharmonic diatomic oscillator model. In this model the bands are pure vibrational overtones of the stretching mode.

The fundamental O–H and O–D stretching frequencies and the three overtones observed and listed in Table 1 permit the calculation of the harmonic oscillator frequency ω_e and the anharmonicity $\omega_e x_e$ for these bonds. We determine Morse potential energy curves with equations [1] to [6] using the nomenclature and approach described in (22). The Morse potential is given by eq. [1] with an equilibrium distance R_e of 0.88 Å (2) for both O–H and O–D oscillators.

$$V(R) = D_e(1 - e^{-\beta(R-R_e)})^2 \qquad [1]$$

The energies of vibrational levels G(v*)* are:

$$\frac{E(v)}{hc} = G(v) = \omega_e(v + \frac{1}{2}) - \omega_e x_e(v + \frac{1}{2})^2 \qquad [2]$$

where v is the vibrational quantum number with values of 0, 1, 2, 3, 4 for our analysis and G(v), ω_e and $\omega_e x_e$ are in wavenumber units. From eq. [2], wavenumber differences ΔG(v+1/2) between any two adjacent vibrational energy levels are calculated as:

$$\Delta G(v + \frac{1}{2}) = (\omega_e - \omega_e x_e) - 2\omega_e x_e(v + \frac{1}{2}) \qquad [3]$$

A Birge-Sponer plot (22) with measured wavenumber differences ΔG(v+1/2) from Table 1 as the ordinate and (v+1/2) as the abscissa is expected to yield a straight line with a slope of $-2\omega_e x_e$. Figure 3 shows these plots including fit lines for $Na_2B(OH)_4Cl$ and $Na_2B(OD)_4Cl$. The resulting parameter values are given in Table 2. The value of ω_e is calculated from the ordinate intercept, ω_e-$\omega_e x_e$, identified in Figure 3, as discussed in detail in (22). The ΔG(v+1/2) values in Figure 3 show a linear decrease, and the choice of the Morse potential appears to be appropriate. Most literature values for ω_e and ω_e-$\omega_e x_e$ for O–H and O–D oscillators are determined from fundamental and first overtone transitions only. The higher overtones reported here allow us to estimate standard deviations, as given in Table 2, using uncertainty propagation starting with the standard deviations of the fitted slopes and ordinate intercepts in Figure 3.

The depth D_e of the Morse potential energy well in wavenumber units is defined by:

$$D_e = \frac{\omega_e^2}{4\omega_e x_e} \qquad [4]$$

The bond dissociation energy D_0 in wavenumber units is:

$$D_0 = \frac{(\omega_e - \omega_e x_e)^2}{4\omega_e x_e} \qquad [5]$$

The β value in cm^{-1} is calculated using eq. (III,100) in (23):

$$\beta = 1.2177 \times 10^7 \omega_e \sqrt{\frac{\mu_A}{D_e}} \qquad [6]$$

μ_A denotes the reduced mass (A: OH^- or OD^-) in g/mol (24). The β values from eq. [6] are converted to more conventional $Å^{-1}$ units in Table 2. Parameter values for the Morse potential in eq. [1], with the exception of R_e, can therefore be determined from the spectra in Figure 2 to within a few percent.

Table 2. Parameters defining anharmonicity and Morse potentials calculated from the peak positions in Table 1.

Parameter	$Na_2B(OH)_4Cl$	$Na_2B(OD)_4Cl$
ω_e (cm^{-1})	3755±18 (±0.5%)	2724±16 (±0.6%)
$\omega_e x_e$ (cm^{-1})	103.5±3.8 (±4%)	53.4±3.5 (±7%)
D_e (cm^{-1})	34058±1292 (±4%)	34739±2313 (±7%)
D_0 (cm^{-1})	32206±1289 (±4%)	33390±2311 (±7%)
β ($Å^{-1}$)	2.41±0.05 (±2%)	2.38±0.08 (±3%)

D_e and β values are expected to be identical for Morse potentials describing OH^- and OD^- bonds. The difference of approximately 2% between the values for $Na_2B(OH)_4Cl$ and $Na_2B(OD)_4Cl$ in Table 2 is within the precision of our data analysis and the Morse curves shown in Figure 4 are nearly identical. D_e values determined from fundamental frequencies and overtones for 17 oxides containing OH^- ions are compiled in (10) using eV units. The values in Table 2 correspond to 4.2±0.2 eV and 4.3±0.3 eV (25), among the lowest four reported in Table 1 of (10). Force constants of 7.9±0.1 mdyn/Å and 7.8±0.1 mdyn/Å are calculated from eq. (III,91) in (23), again matching for teepleite and its deutero analog.

The D_0 values in Table 2 correspond to bond dissociation energies of 385±15 kJ/mol and 399±28 kJ/mol, for OH^- and OD^-, respectively (26). They are lower by approximately 15% than the textbook value of 459 kJ/mol for the average O–H bond (27) but within 5% of the 424±2 kJ/mol gas phase bond dissociation energy of the OH radical (28). This overall agreement is satisfactory. The D_0 value for $Na_2B(OD)_4Cl$ in Table 2 is higher by 14 kJ/mol than for

$Na_2B(OH)_4Cl$, due to the lower vibrational frequency of the deutero analog, but this difference has a very significant error from the uncertainties of the bond dissociation energies. Nevertheless, it is comparable to the difference of the zero-point vibrational energies of 6.0±0.1 kJ/mol, calculated with eq. [2]. The ratios of ω_e and $\omega_e x_e$ for $Na_2B(OD)_4Cl$ and $Na_2B(OH)_4Cl$ from Table 2 are 0.725±0.005 and 0.52±0.04, respectively, in excellent agreement with the expected ratios of 0.728 and 0.53 (29).

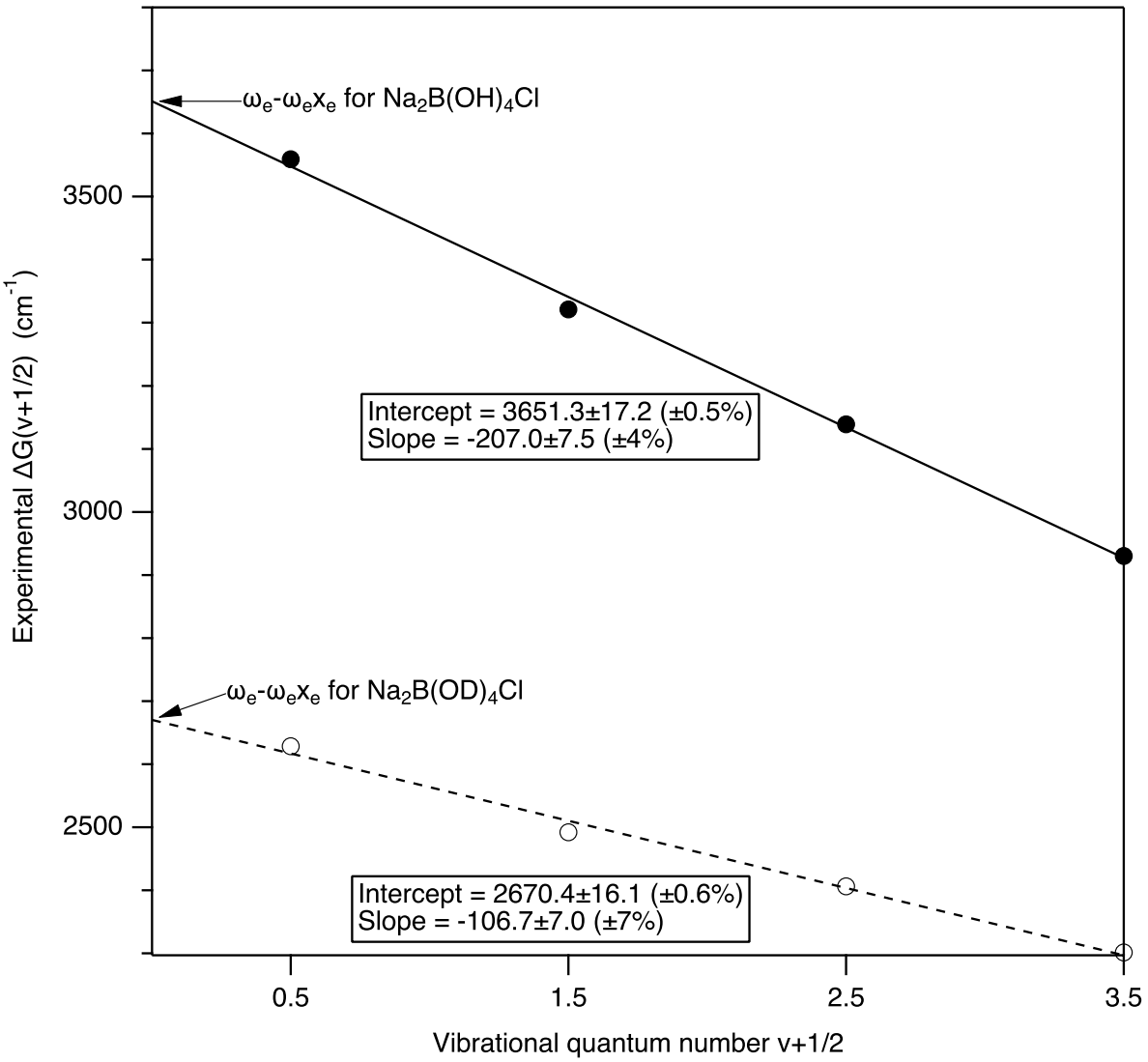

Figure 3. Birge-Sponer plot of observed wavenumber differences ΔG(v+1/2) for $Na_2B(OH)_4Cl$ and $Na_2B(OD)_4Cl$ from Table 1. Solid circles: undeuterated teepleite, open circles: deuterated teepleite. Solid and dotted lines are least-squares fits to ΔG(v+1/2) values from the spectra of the undeuterated and deuterated crystals, respectively. Parameter values calculated from the fits are given in Table 2.

Calculated Morse curves with vibrational energy levels, transitions and intervals ΔG(v+1/2) used to analyze the spectra in Figure 2 are shown in Figure 4. The ordinate range is chosen from the potential energy minima throughout the approximate wavenumber range of the spectra in Figure 2.

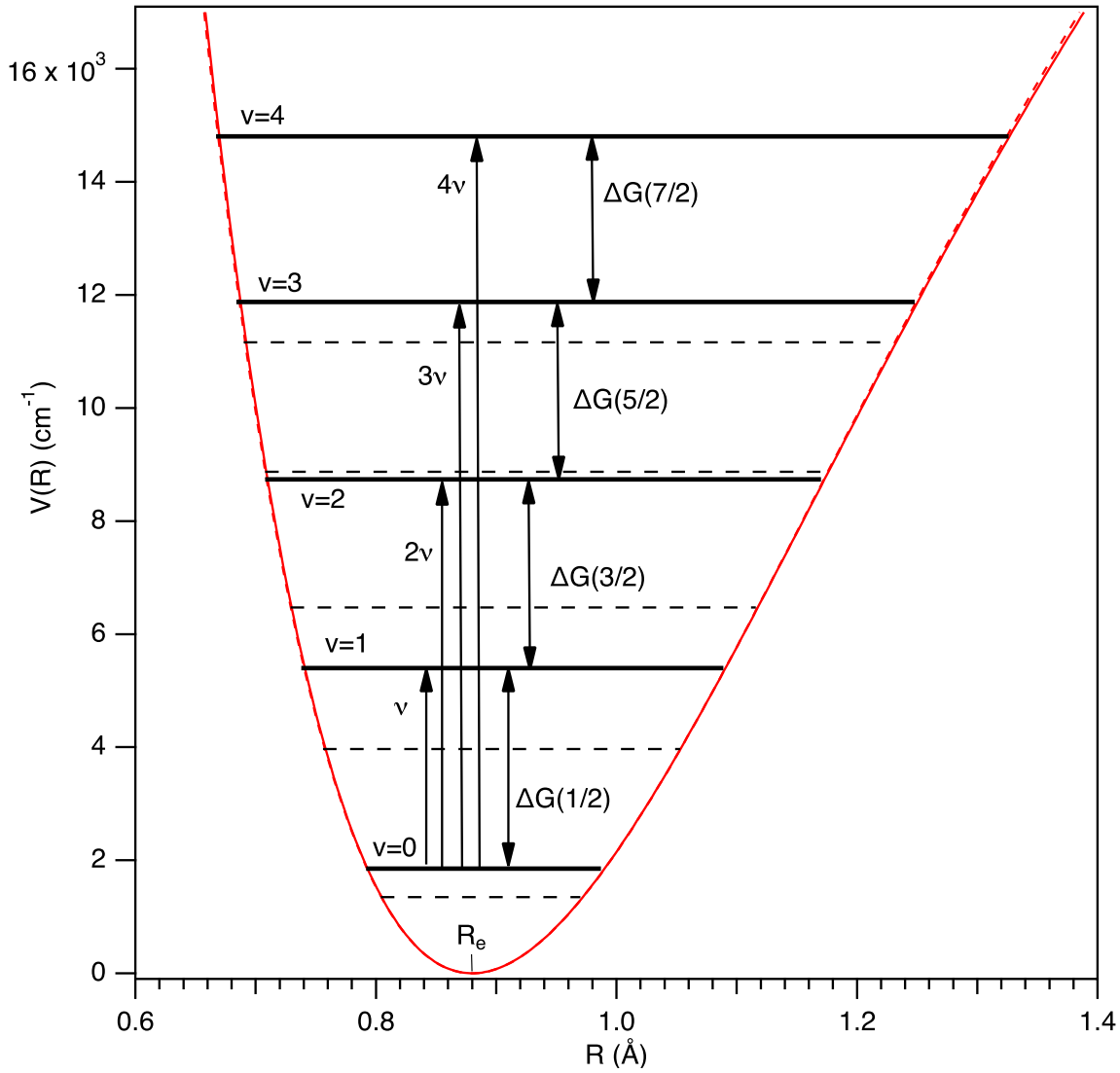

Figure 4. Morse potential energy curves calculated from eq. [1] with the parameter values in Table 2 and an R_e value of 0.88 Å. The solid and dotted curves obtained for $Na_2B(OH)_4Cl$ and $Na_2B(OD)_4Cl$ are almost identical. Solid and dotted horizontal lines denote energy levels for O–H and O–D oscillators, respectively, calculated from eq. [2]. Quantum numbers v for each O–H level are given. Fundamental and overtone transitions for the O–H oscillator are shown as vertical arrows. Wavenumber differences ΔG(v+1/2) between adjacent energy levels are denoted by vertical double arrows.

Table 3 lists the ω_e and $\omega_e x_e$ values calculated for teepleite and reported for other O–H and O–D oscillators.

Table 3. Harmonic frequencies ω_e and anharmonicities $\omega_e x_e$ for selected O-H and O-D oscillators.

Compound	ω_e (cm^{-1})	$\omega_e x_e$ (cm^{-1})
$Na_2B(OH)_4Cl$[a]	3755±18	104±4
OH(g) radical[b]	3735.2	82.8
Cd(OH)Cl[c]	3704	93
Sr(OH)Cl[c]	3752	86
OH^- in KBr[d]	3789	85.5
$Mg(OH)_2$ [c]	3871	98
$Ca(OH)_2$[c]	3814	91
$Mn(OH)_2$[c]	3797	98
$Fe(OH)_2$[c]	3794	97
$Co(OH)_2$[c]	3799	100
$Ni(OH)_2$[c]	3813	102
CD_3OH/CD_3OD[e]	3340	115
$Na_2B(OD)_4Cl$[a]	2724±16	53±4
OD(g) radical[b]	2720.9	44.2
$Ca(OD)_2$[c]	2765	45
$Fe(OD)_2$[c]	2758	51

[a] This work. Fundamental and three overtone bands observed and used for the analysis.
[b] From (23), p. 560.
[c] From (14). Fundamental and first overtone transitions reported. The average of the observed Raman and IR fundamental bands in polycrystalline samples at room temperature was used. Calculated ω_e and $\omega_e x_e$ values rounded to integer wavenumber values.
[d] From (13). Fundamental and first overtone measured at 78 K for a KBr crystal doped with KOH.
[e] From (12).

The harmonic frequencies ω_e for teepleite and its deuterated analog are similar to those for the OH and OD radicals in the gas phase. Solids with O–H···Cl hydrogen bonding, such as Cd(OH)Cl and Sr(OH)Cl also show similar, possibly slightly lower ω_e values. The lowest values are reported for organic O-H bonds in compounds with strong hydrogen bonding. In contrast, hydroxide ions in doped crystals and in a series of brucites of general formula $M(OH)_2$ show higher ω_e values than teepleite, indicative of the absence of hydrogen bonding. Variations of ω_e for deuterated systems are smaller, but appear to be in line with the same qualitative trends.

The $\omega_e x_e$ values determined here for teepleite are among the highest reported for inorganic solids and comparable to those for organic O-H bonds, higher by approximately 20% than for the corresponding gas-phase radicals. This increase can be ascribed to the influence of hydrogen

bonding, as has been discussed in detail for organic hydrogen-bonded systems (12). Values for the solids in the $M(OH)_2$ series in Table 3 show significant variations, not easily correlated to a single physical origin. A comparison of $\omega_e x_e$ values plotted as a function of ω_e for more than 150 oxide and alkali halide compounds containing OH^- impurities confirms the general trend of decreasing anharmonicity with increasing harmonic frequency (10). Deuterated systems show variations of $\omega_e x_e$ that are most likely smaller than the experimental precision of the spectroscopic data.

Teepleite and its deuterated analog allow us to apply the textbook anharmonic model for diatomic oscillators based on Morse potential energy curves. The three exceptionally intense, sharp overtone transitions provide the experimental information needed to calculate the anharmonicity of O–H and O–D oscillators in a crystalline environment with extended hydrogen bonding and to estimate the uncertainty of the resulting parameters. The NIR absorption spectra contribute to our understanding of isotope effects in hydrogen-bonded systems, and more generally also to acid-base reactions and proton-coupled electron transfer processes.

Acknowledgements

PJM thanks the Research Corporation for assistance in purchasing the Displex Cryogenic Refrigerator. IMW and CR thank the Natural Sciences and Engineering Research Council of Canada for financial support. We thank Rémi Beaulac, Guillaume Bussière and Christian Pellerin for helpful comments and careful proofreading of this report.

References

1. https://www.mindat.org/min-3901.html (accessed December 5, 2021).
2. Effenberger, H., *Acta Cryst.* **1982,** *B38*, 82.
3. Walker, I. M.; McCarthy, P. J., *Can. J. Chem.* **1994,** *72*, 1211.
4. Walker, I. M.; McCarthy, P. J., *Can. J. Chem.* **1996,** *74*, 246.
5. McCarthy, P. J.; Lauffenburger, J. C.; Schreiner, M. M.; Rohrer, D. C., *Inorg. Chem.* **1981,** *20*, 1566.
6. McCarthy, P. J.; Lauffenburger, J. C.; Schreiner, M. M.; Rohrer, D. C., *Inorg. Chem.* **1981,** *20*, 1571.
7. Devarajan, V.; Gräfe, E.; Funck, E., *Spectrochim. Acta* **1974,** *30A*, 1235.
8. Klee, W. E., *Z. Anorg. Allg. Chem.* **1966,** *343*, 58.
9. Hermansson, K.; Probst, M. M.; Gajewski, G.; Mitev, P. D., *J. Chem. Phys.* **2009,** *131*, 244517.
10. Wöhlecke, M.; Kovács, L., *Crit. Rev. Solid State Mater. Sci.* **2001,** *26*, 1.
11. Otto, S.; Dorn, M.; Förster, C.; Bauer, M.; Seitz, M.; Heinze, K., *Coord. Chem. Rev.* **2018,** *359*, 102.
12. Sandorfy, C., Anharmonicity and Hydrogen Bonding. In *The Hydrogen Bond*, Schuster, P.; Zundel, G.; Sandorfy, C., Eds. North Holland: Amsterdam, New York, Oxford, 1976; Vol.II, p 613 and references therein.
13. Wedding, B.; Klein, M. V., *Phys. Rev.* **1969,** *177*, 1274.
14. Weckler, B.; Lutz, H. D., *Spectrochim. Acta* **1996,** *A52*, 1507.
15. McCarthy, P. J.; Walker, I. M., *Spectrochim. Acta* **1983,** *39A*, 827.
16. Walker, I. M.; McCarthy, P. J., *Can. J. Chem.* **1986,** *64*.
17. Walker, I. M.; McCarthy, P. J., *J. Phys. Chem.* **1989,** *93*, 2230.
18. McCarthy, P. J.; Walker, I. M., *Inorg. Chem.* **1990,** *29*, 820.
19. McCarthy, P. J.; Walker, I. M., *Inorg. Chem.* **1991,** *30*, 2772.
20. Walker, I. M.; McCarthy, P. J., *Can. J. Chem.* **1997,** *75*, 1099.
21. Harris, D. C.; Bertolucci, M. D., *Symmetry and Spectroscopy*. Oxford University Press: 1978.
22. Lessinger, L., *J. Chem. Ed.* **1994,** *71*, 388 and references therein.
23. Herzberg, G., *Molecular Spectra and Molecular Structure I. Spectra of Diatomic Molecules*. Second ed.; D. Van Nostrand Company, Inc.: Toronto, New York, London, 1950.
24. Atomic masses of 1.007825 g/mol, 2.0141082 g/mol and 15.999 g/mol were used for H, D, and O, leading to reduced masses μ_{OH} and μ_{OD} of 0.94810 g/mol and 1.78890 g/mol, respectively.
25. 1 cm^{-1} = 1.2399 × 10^{-4} eV from Appendix F of (21)
26. 1 cm^{-1} = 11.963 J/mol from Appendix F of (21)
27. Huheey, J. E.; Keiter, E. A.; Keiter, R. L., *Inorganic Chemistry*. Fourth ed.; HarperCollins College Publishers: New York, 1993, Table E.1, page A-25.
28. Darwent, B. d. B., *Bond Dissociation Energies in Simple Molecules*. Nat. Bur. Stand. (U.S.): Washington, DC, 1970; Vol. 31, p 41.
29. $\omega_{e,OD}/\omega_{e,OH} = (\mu_{OH}/\mu_{OD})^{1/2}$ from eq. (III,33) in (23). $\omega_{e,OD}x_{e,OD}/\omega_{e,OH}x_{e,OH} = \mu_{OH}/\mu_{OD}$ from eq. 6 in (22) with μ the reduced mass in g/mol given in (24).